

# The *E. coli* molecular phenotype under different growth conditions

## Supplementary materials

Mehmet U. Caglar\*, John R. Houser, Craig S. Barnhart,  
Daniel R. Boutz, Sean M. Carroll, Aurko Dasgupta, Walter F. Lenoir,  
Bartram L. Smith, Viswanadham Sridhara, Dariya K. Sydykova,  
Drew Vander Wood, Christopher J. Marx,  
Edward M. Marcotte\*, Jeffrey E. Barrick\*, Claus O. Wilke\*

January 30, 2017

## List of Figures

S1	Significantly differentially expressed molecular functions . . . . .	4
S2	Significantly differentially expressed KEGG pathways for mRNA samples in exponential phase tested for glycerol against glucose . . . . .	5
S3	Significantly differentially expressed KEGG pathways for mRNA samples in exponential phase tested for gluconate against glucose . . . . .	6
S4	Significantly differentially expressed KEGG pathways for mRNA samples in exponential phase tested for lactate against glucose . . . . .	7
S5	Significantly differentially expressed KEGG pathway for protein samples in exponential phase tested for gluconate against glucose . . . . .	8
S6	Significantly differentially expressed KEGG pathways for protein samples in exponential phase tested for lactate against glucose . . . . .	9
S7	Significantly differentially expressed KEGG pathway for protein samples in stationary phase tested for glycerol against glucose . . . . .	10
S8	Significantly differentially expressed KEGG pathway for protein samples in stationary phase tested for gluconate against glucose . . . . .	11
S9	Significantly differentially expressed KEGG pathways for protein samples in stationary phase tested for lactate against glucose . . . . .	12
S10	Significantly differentially expressed KEGG pathways for mRNA samples in exponential phase tested for low $Mg^{2+}$ levels against base $Mg^{2+}$ . . . . .	13
S11	Significantly differentially expressed KEGG pathways for mRNA samples in exponential phase tested for high $Mg^{2+}$ against base $Mg^{2+}$ . . . . .	14
S12	Significantly differentially expressed KEGG pathways for protein samples in exponential phase tested for high $Mg^{2+}$ against base $Mg^{2+}$ . . . . .	15
S13	Significantly differentially expressed KEGG pathway for mRNA samples in stationary phase tested for high $Mg^{2+}$ against base $Mg^{2+}$ . . . . .	16
S14	Significantly differentially expressed KEGG pathway for mRNA samples in exponential phase tested for high $Na^+$ against base $Na^+$ . . . . .	17
S15	Significantly differentially expressed KEGG pathways for protein samples in exponential phase tested for high $Na^+$ against base $Na^+$ . . . . .	18
S16	Significantly differentially expressed KEGG pathways for mRNA samples in stationary phase tested for high $Na^+$ against base $Na^+$ . . . . .	19
S17	Significantly differentially expressed KEGG pathways for protein samples in stationary phase tested for high $Na^+$ against base $Na^+$ . . . . .	20
S18	Significantly differentially expressed GO annotations associated with molecular functions for mRNA samples in exponential phase tested for glycerol against glucose . . . . .	21
S19	Significantly differentially expressed GO annotations associated with molecular functions for mRNA samples in exponential phase tested for gluconate against glucose . . . . .	21
S20	Significantly differentially expressed GO annotations associated with molecular functions for mRNA samples in exponential phase tested for lactate against glucose . . . . .	22
S21	Significantly differentially expressed GO annotations associated with molecular functions for protein samples in exponential phase tested for glycerol against glucose . . . . .	22
S22	Significantly differentially expressed GO annotations associated with molecular functions for protein samples in exponential phase tested for lactate against glucose . . . . .	23
S23	Significantly differentially expressed GO annotations associated with molecular functions for protein samples in stationary phase tested for glycerol against glucose . . . . .	23
S24	Significantly differentially expressed GO annotations associated with molecular functions for protein samples in stationary phase tested for gluconate against glucose . . . . .	24
S25	Significantly differentially expressed GO annotations associated with molecular functions for protein samples in stationary phase tested for lactate against glucose . . . . .	24
S26	Significantly differentially expressed GO annotations associated with molecular functions for mRNA samples in exponential phase tested for low $Mg^{2+}$ levels against base $Mg^{2+}$ levels . . . . .	25
S27	Significantly differentially expressed GO annotations associated with molecular functions for mRNA samples in exponential phase tested for high $Mg^{2+}$ levels against base $Mg^{2+}$ levels . . . . .	25

S28	Significantly differentially expressed GO annotations associated with molecular functions for protein samples in exponential phase tested for low $\text{Mg}^{2+}$ levels against base $\text{Mg}^{2+}$ levels	26
S29	Significantly differentially expressed GO annotations associated with molecular functions for protein samples in exponential phase tested for high $\text{Mg}^{2+}$ levels against base $\text{Mg}^{2+}$ levels . . . . .	26
S30	Significantly differentially expressed GO annotations associated with molecular functions for mRNA samples in stationary phase tested for low $\text{Mg}^{2+}$ levels against base $\text{Mg}^{2+}$ levels	27
S31	Significantly differentially expressed GO annotations associated with molecular functions for protein samples in exponential phase tested for high $\text{Na}^+$ levels against base $\text{Na}^+$ levels	27
S32	Significantly differentially expressed GO annotations associated with molecular functions for mRNA samples in stationary phase tested for high $\text{Na}^+$ levels against base $\text{Na}^+$ levels	28
S33	Significantly differentially expressed GO annotations associated with molecular functions for protein samples in stationary phase tested for high $\text{Na}^+$ levels against base $\text{Na}^+$ levels	28
S34	Fraction of differentially expressed genes that are found in analyses with or without controlling for doubling time . . . . .	29
S35	Flux ratios versus ion concentrations . . . . .	30

## Supplementary Figures

A	mRNA	Protein	
	1.structural constituent of ribosome ▼▼▼ 2.rRNA binding ▼▼▼ 3.structural molecule activity ▼▼▼ 4.RNA binding ▼▼▼ 5.RNA-dependent ATPase activity ▼▼▼	1.L-lactate dehydrogenase activity ▼▼▼ 2.lactate dehydrogenase activity ▼▼▼	lowMg
	1.energy transducer activity ▲ 2.alkanesulfonate transporter activity ▲ 3.oxidoreductase activity ▲▼	1.L-lactate dehydrogenase activity ▼▼▼ 2.lactate dehydrogenase activity ▼▼▼	highMg
		1.binding ▼ 2.protein binding ▼ 3.structural constituent of ribosome ▼▼▼ 4.small molecule binding ▼ 5.nucleotide binding ▼	highNa
	1.structural constituent of ribosome ▼▼▼ 2.structural molecule activity ▼▼▼ 3.rRNA binding ▼▼▼ 4.RNA binding ▼▼▼ 5.tRNA binding ▼▼▼	1.ATP binding ▼▼ 2.adenyl ribonucleotide binding ▼▼ 3.adenyl nucleotide binding ▼▼ 4.molecular transducer activity ▼▼▼ 5.oxidoreductase activity, acting on the CH-OH group of donors, quinon	glycerol
	1.gluconate transmembrane transporter activity ▲ 2.aldonate transmembrane transporter activity ▲		gluconate
	1.structural constituent of ribosome ▲▲ 2.structural molecule activity ▲▲ 3.rRNA binding ▲▲ 4.RNA binding ▲▲ 5.lactate dehydrogenase activity ▲▲	1.catalytic activity ▲▲ 2.lactate dehydrogenase activity ▲▲ 3.hydrolase activity ▲▲ 4.L-lactate dehydrogenase activity ▲▲	lactate
B	mRNA	Protein	
	1.ATPase activity ▼▼▼ 2.hydrolase activity, acting on acid anhydrides, catalyzing transmembr 3.oligopeptide-transporting ATPase activity ▼▼▼ 4.peptide-transporting ATPase activity ▼▼▼ 5.ATPase activity, coupled ▼▼▼		lowMg
			highMg
	1.carbohydrate transmembrane transporter activity ▼▼ 2.carbohydrate transporter activity ▼▼ 3.polyol transmembrane transporter activity ▼▼ 4.alcohol transmembrane transporter activity ▼▼ 5.organic hydroxy compound transmembrane transporter activity ▼▼▼	1.protein binding ▼ 2.binding ▼ 3.structural constituent of ribosome ▼▼▼ 4.ion binding ▼ 5.structural molecule activity ▼▼▼	highNa
		1.oxidoreductase activity ▼▼ 2.oxidoreductase activity, acting on the aldehyde or oxo group of donors 3.coenzyme binding ▼ 4.oxidoreductase activity, acting on the CH-OH group of donors, quinon 5.cofactor binding ▼	glycerol
		1.siderophore transmembrane transporter activity ▼▼▼ 2.2,3-dihydroxybenzoate-serine ligase activity ▼▼▼ 3.siderophore transporter activity ▼▼▼ 4.iron chelate transmembrane transporter activity ▼▼▼	gluconate
		1.lactate dehydrogenase activity ▲▲ 2.oxidoreductase activity, acting on CH-OH group of donors ▲▲ 3.binding ▲▲ 4.L-lactate dehydrogenase activity ▲▲ 5.cofactor binding ▲▲	lactate

Figure S1: **Significantly differentially expressed molecular functions, as determined by GO annotations.** For each condition, we show the top-5 differentially expressed molecular functions according to either mRNA or protein abundances. Empty boxes indicate that no differentially expressed pathways were found. The arrows next to pathway names indicate the proportion of up- and down-regulated genes among the significantly differentially expressed genes in this pathway. One up arrow indicates that 60% or more of the genes are up-regulated, two arrows correspond to 80% or more genes, and three arrows correspond to 95% or more genes being up-regulated. Similarly, down arrows indicate the proportion of down-regulated genes. (A) Exponential phase. (B) Stationary phase.

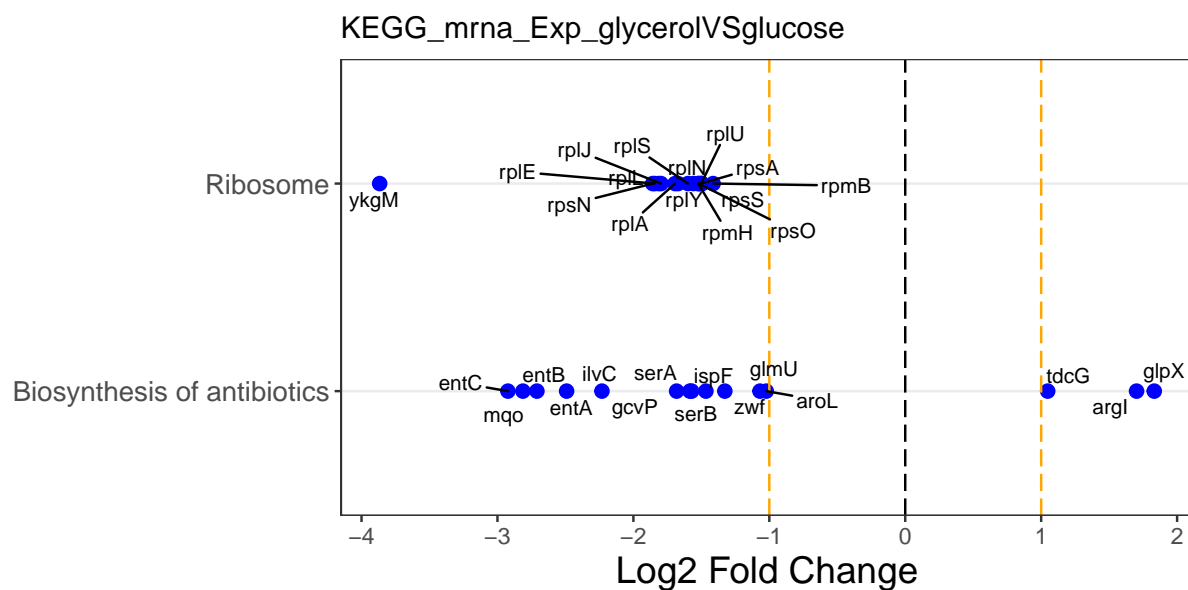


Figure S2: **Significantly differentially expressed KEGG pathways and associated genes with glycerol as carbon source, as determined by mRNA abundances in exponential phase.** The top 2 differentially expressed KEGG pathways are shown along the  $y$  axis, and the relative fold change of the corresponding genes is shown along the  $x$  axis. We show up to 10 of the most significantly changed pathways and for each pathway we show up to 15 of the most significantly changing genes.

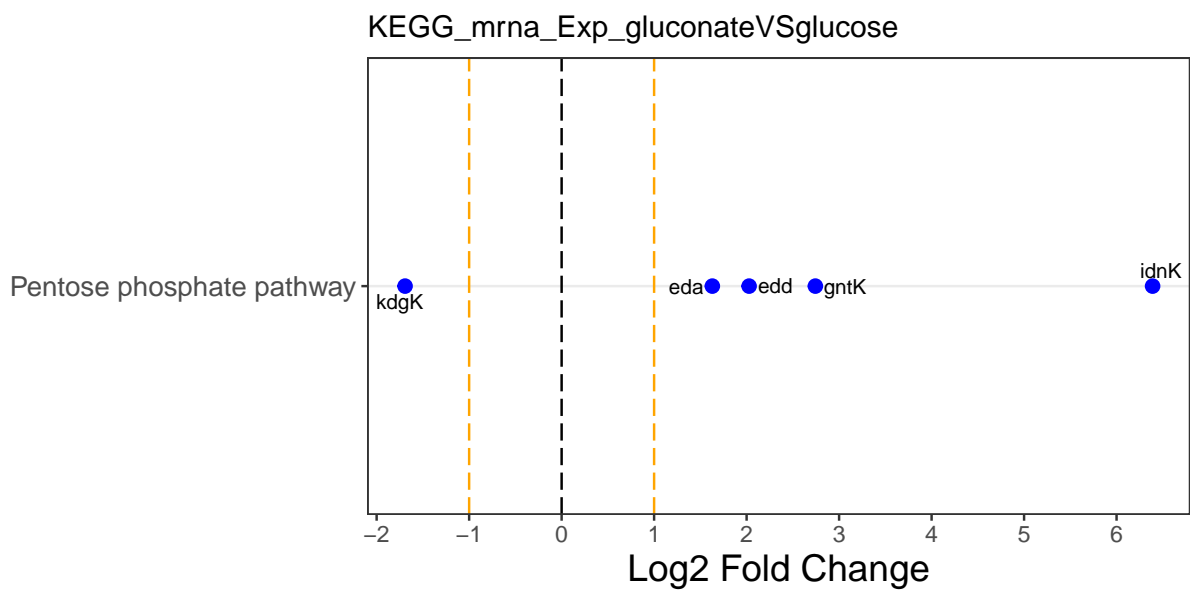


Figure S3: **Significantly differentially expressed KEGG pathway and associated genes with gluconate as carbon source, as determined by mRNA abundances in exponential phase.** The top differentially expressed KEGG pathway is shown along the  $y$  axis, and the relative fold change of the corresponding genes is shown along the  $x$  axis. We show up to 10 of the most significantly changed pathways and for each pathway we show up to 15 of the most significantly changing genes.

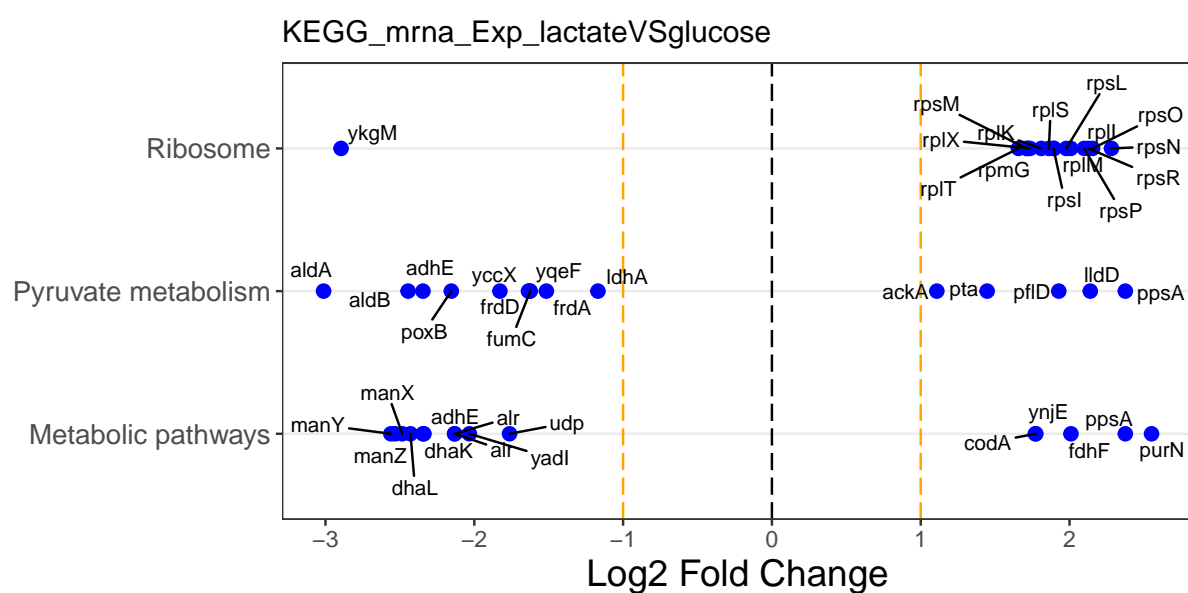


Figure S4: **Significantly differentially expressed KEGG pathways and associated genes with lactate as carbon source, as determined by mRNA abundances in exponential phase.** The top 3 differentially expressed KEGG pathways are shown along the  $y$  axis, and the relative fold change of the corresponding genes is shown along the  $x$  axis. We show up to 10 of the most significantly changed pathways and for each pathway we show up to 15 of the most significantly changing genes.

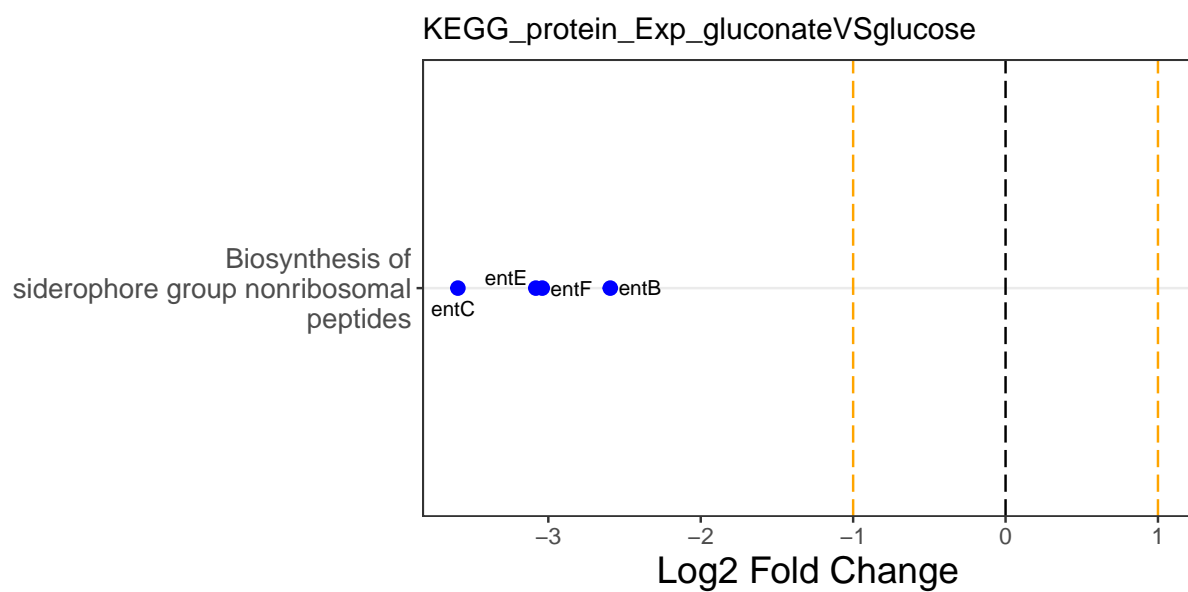


Figure S5: **Significantly differentially expressed KEGG pathway and associated genes with gluconate as carbon source, as determined by protein abundances in exponential phase.** The top differentially expressed KEGG pathway is shown along the  $y$  axis, and the relative fold change of the corresponding genes is shown along the  $x$  axis. We show up to 10 of the most significantly changed pathways and for each pathway we show up to 15 of the most significantly changing genes.



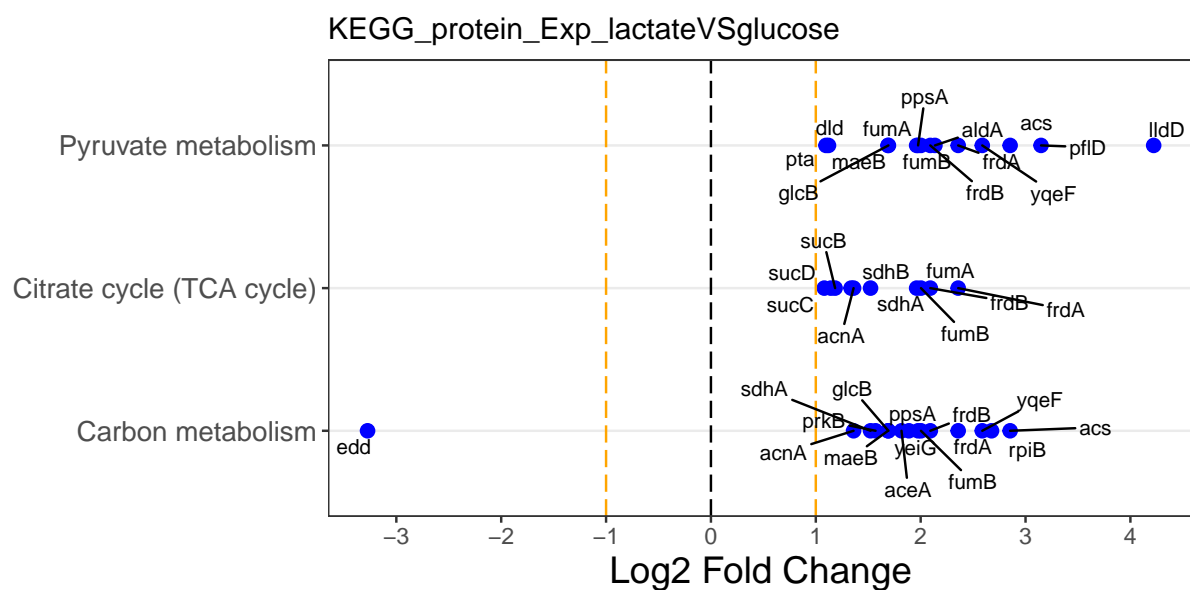


Figure S6: **Significantly differentially expressed KEGG pathways and associated genes with lactate as carbon source, as determined by protein abundances in exponential phase.** The top 3 differentially expressed KEGG pathways are shown along the  $y$  axis, and the relative fold change of the corresponding genes is shown along the  $x$  axis. We show up to 10 of the most significantly changed pathways and for each pathway we show up to 15 of the most significantly changing genes.

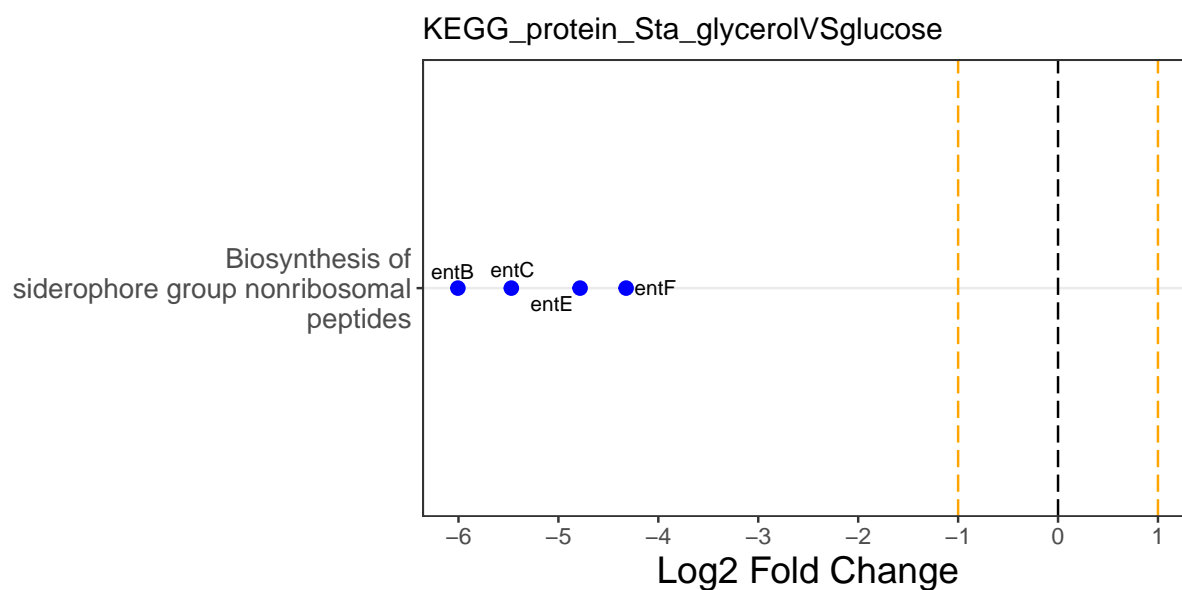


Figure S7: **Significantly differentially expressed KEGG pathway and associated genes with glycerol as carbon source, as determined by protein abundances in stationary phase.** The top differentially expressed KEGG pathway is shown along the  $y$  axis, and the relative fold change of the corresponding genes is shown along the  $x$  axis. We show up to 10 of the most significantly changed pathways and for each pathway, we show up to 15 of the most significantly changing genes.

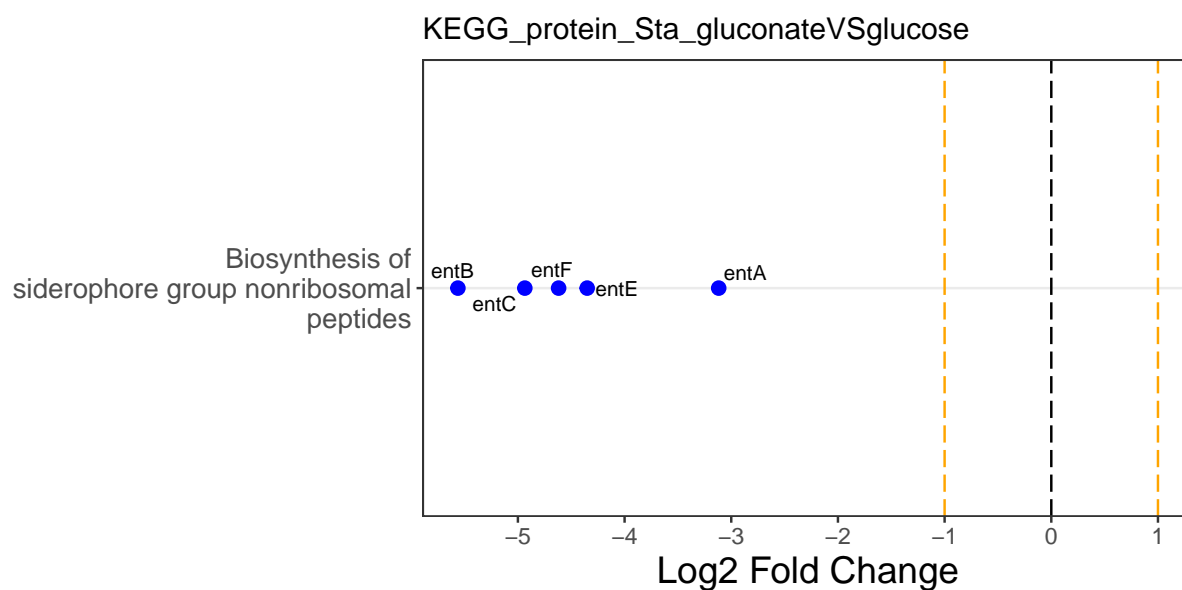


Figure S8: **Significantly differentially expressed KEGG pathway and associated genes with gluconate as carbon source, as determined by protein abundances in stationary phase.** The top differentially expressed KEGG pathway is shown along the  $y$  axis, and the relative fold change of the corresponding genes is shown along the  $x$  axis. We show up to 10 of the most significantly changed pathways and for each pathway, we show up to 15 of the most significantly changing genes.

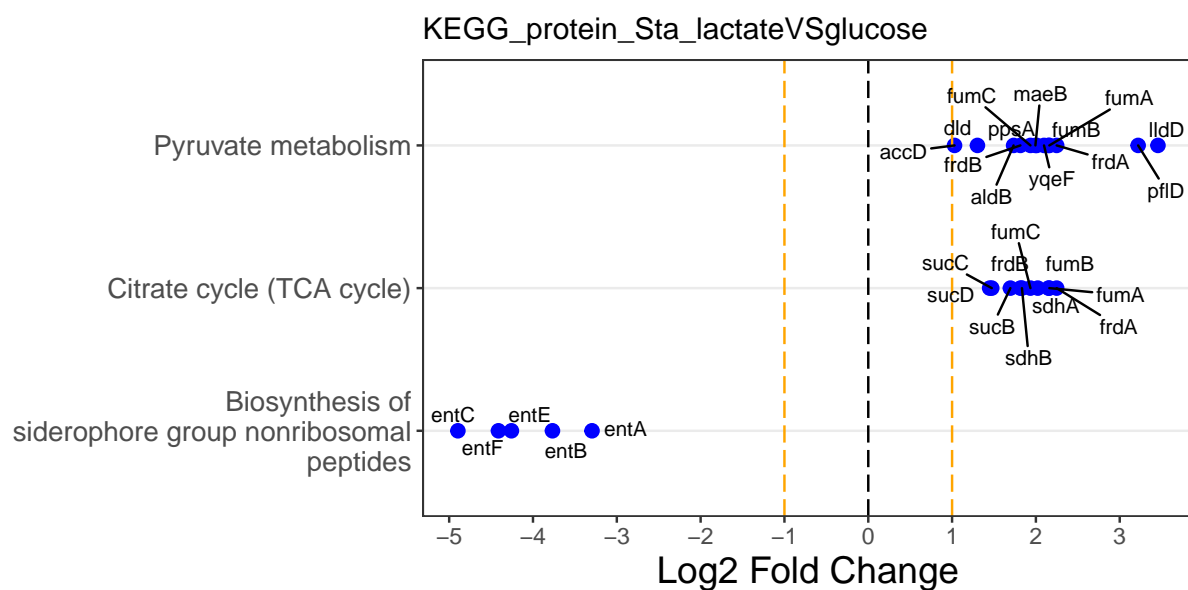


Figure S9: **Significantly differentially expressed KEGG pathways and associated genes with lactate as carbon source, as determined by protein abundances in stationary phase.** The top 3 differentially expressed KEGG pathways are shown along the  $y$  axis, and the relative fold change of the corresponding genes is shown along the  $x$  axis. We show up to 10 of the most significantly changed pathways and for each pathway, we show up to 15 of the most significantly changing genes.

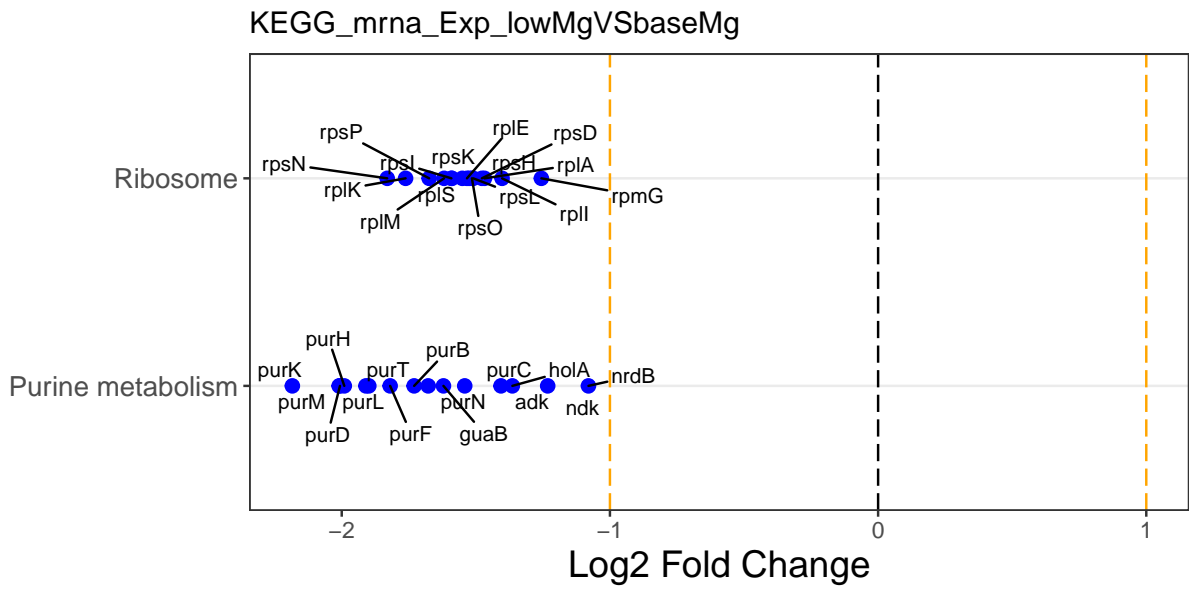


Figure S10: **Significantly differentially expressed KEGG pathways and associated genes with low  $Mg^{2+}$  levels, as determined by mRNA abundances in exponential phase.** The top 2 differentially expressed KEGG pathways are shown along the  $y$  axis, and the relative fold change of the corresponding genes is shown along the  $x$  axis. We show up to 10 of the most significantly changed pathways and for each pathway, we show up to 15 of the most significantly changing genes.

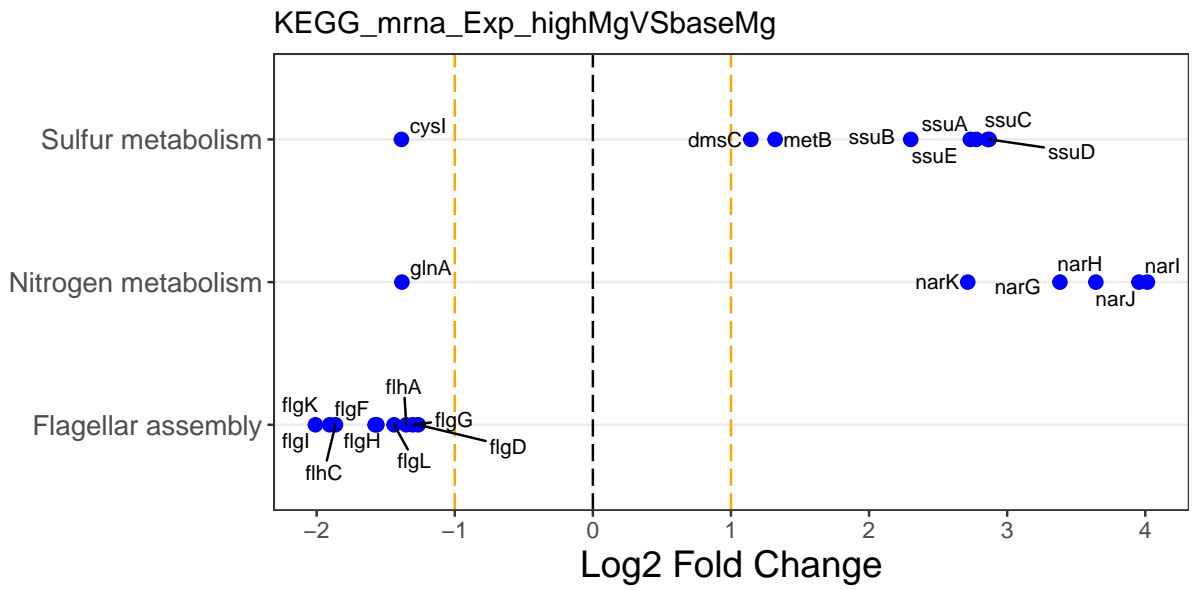


Figure S11: **Significantly differentially expressed KEGG pathways and associated genes with high  $\text{Mg}^{2+}$  levels, as determined by mRNA abundances in exponential phase.** The top 3 differentially expressed KEGG pathways are shown along the  $y$  axis, and the relative fold change of the corresponding genes is shown along the  $x$  axis. We show up to 10 of the most significantly changed pathways and for each pathway, we show up to 15 of the most significantly changing genes.

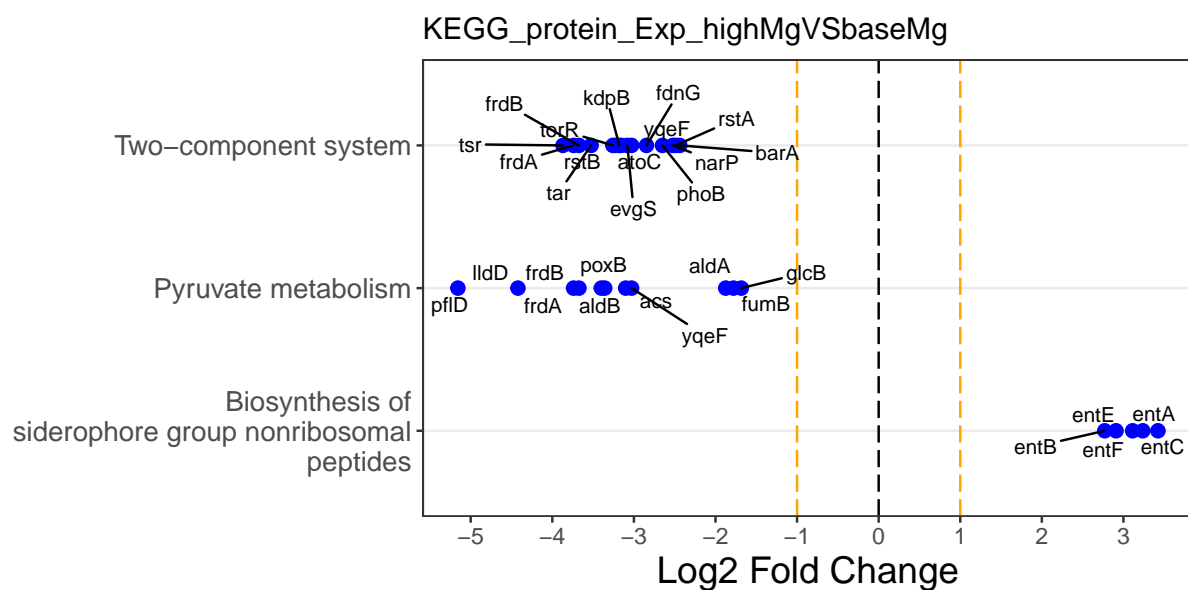


Figure S12: **Significantly differentially expressed KEGG pathways and associated genes with high  $\text{Mg}^{2+}$  levels, as determined by protein abundances in exponential phase.** The top 3 differentially expressed KEGG pathways are shown along the  $y$  axis, and the relative fold change of the corresponding genes is shown along the  $x$  axis. We show up to 10 of the most significantly changed pathways and for each pathway, we show up to 15 of the most significantly changing genes.

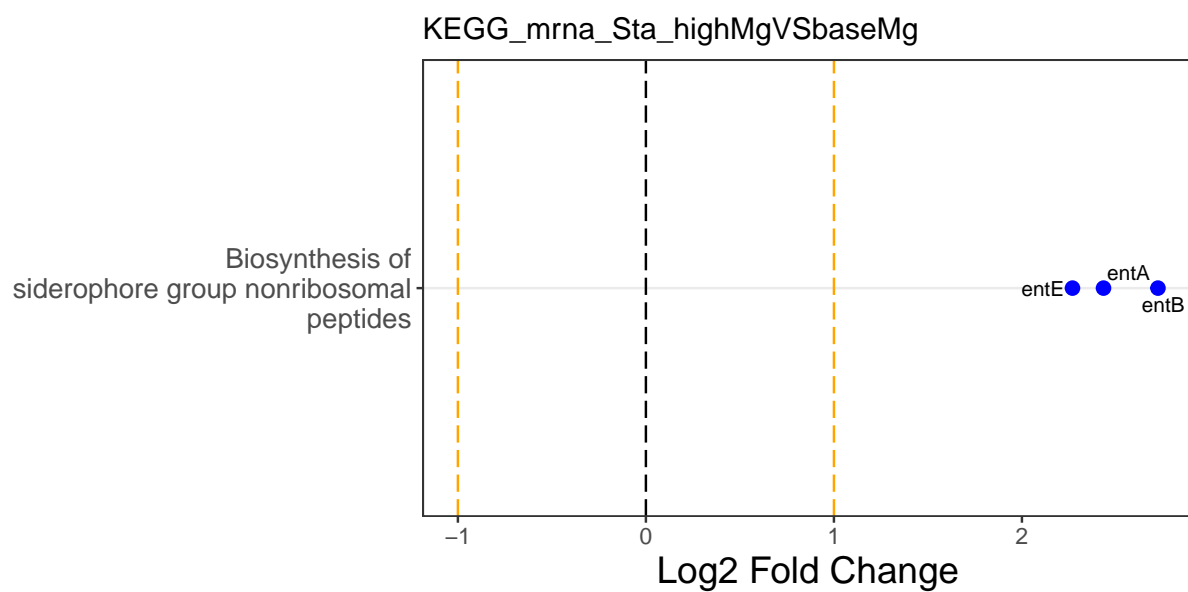


Figure S13: **Significantly differentially expressed KEGG pathway and associated genes with high  $\text{Mg}^{2+}$  levels, as determined by mRNA abundances in stationary phase.** The top differentially expressed KEGG pathway is shown along the  $y$  axis, and the relative fold change of the corresponding genes is shown along the  $x$  axis. We show up to 10 of the most significantly changed pathways and for each pathway, we show up to 15 of the most significantly changing genes.



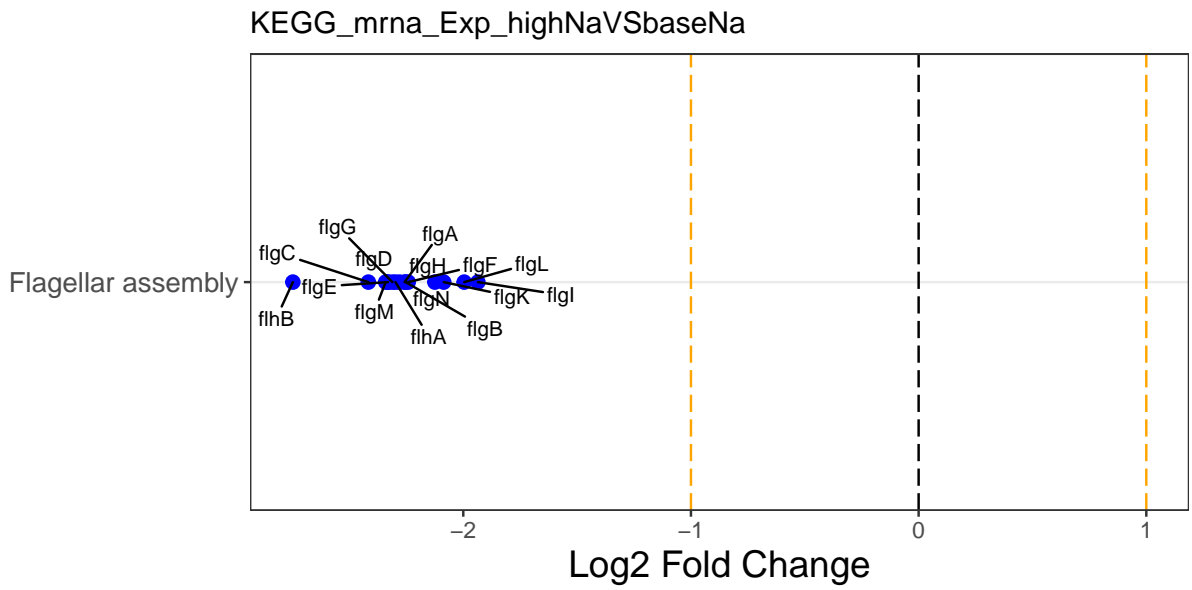


Figure S14: **Significantly differentially expressed KEGG pathway and associated genes with high  $\text{Na}^+$  levels, as determined by mRNA abundances in exponential phase.** The top differentially expressed KEGG pathway is shown along the  $y$  axis, and the relative fold change of the corresponding genes is shown along the  $x$  axis. We show up to 10 of the most significantly changed pathways and for each pathway, we show up to 15 of the most significantly changing genes.

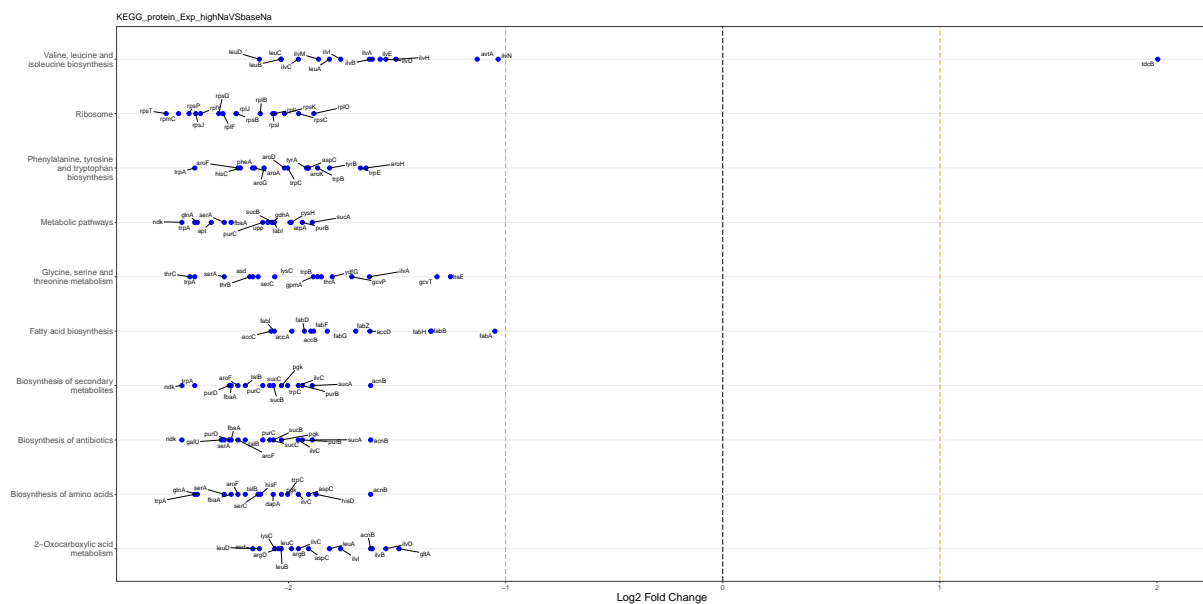


Figure S15: **Significantly differentially expressed KEGG pathways and associated genes with high  $\text{Na}^+$  levels, as determined by protein abundances in exponential phase.** The top 10 differentially expressed KEGG pathways are shown along the  $y$  axis, and the relative fold change of the corresponding genes is shown along the  $x$  axis. We show up to 10 of the most significantly changed pathways and for each pathway, we show up to 15 of the most significantly changing genes.

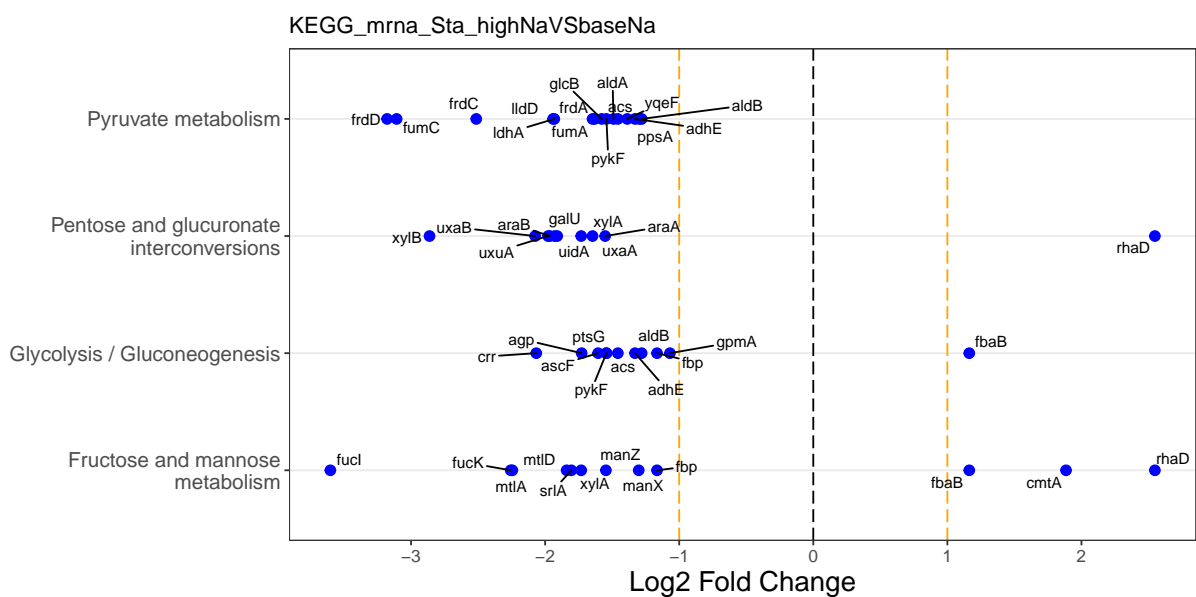


Figure S16: **Significantly differentially expressed KEGG pathways and associated genes with high  $\text{Na}^+$  levels, as determined by mRNA abundances in stationary phase.** The top 4 differentially expressed KEGG pathways are shown along the  $y$  axis, and the relative fold change of the corresponding genes is shown along the  $x$  axis. We show up to 10 of the most significantly changed pathways and for each pathway, we show up to 15 of the most significantly changing genes.

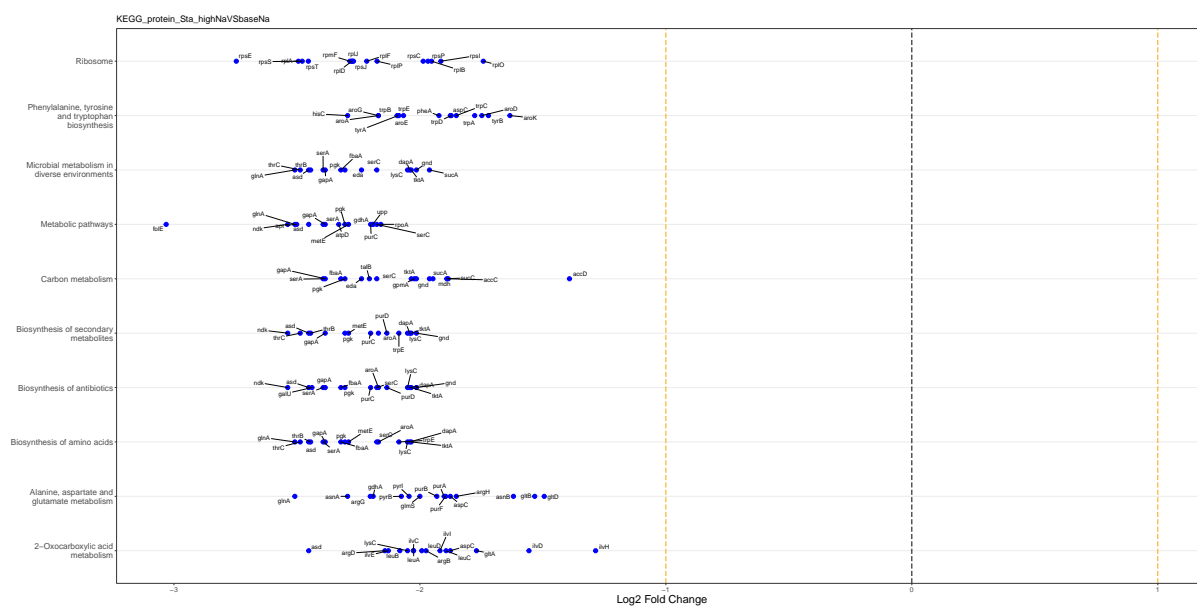


Figure S17: **Significantly differentially expressed KEGG pathways and associated genes with high Na<sup>+</sup> levels, as determined by protein abundances in stationary phase.** The top 10 differentially expressed KEGG pathways are shown along the *y* axis, and the relative fold change of the corresponding genes is shown along the *x* axis. We show up to 10 of the most significantly changed pathways and for each pathway, we show up to 15 of the most significantly changing genes.





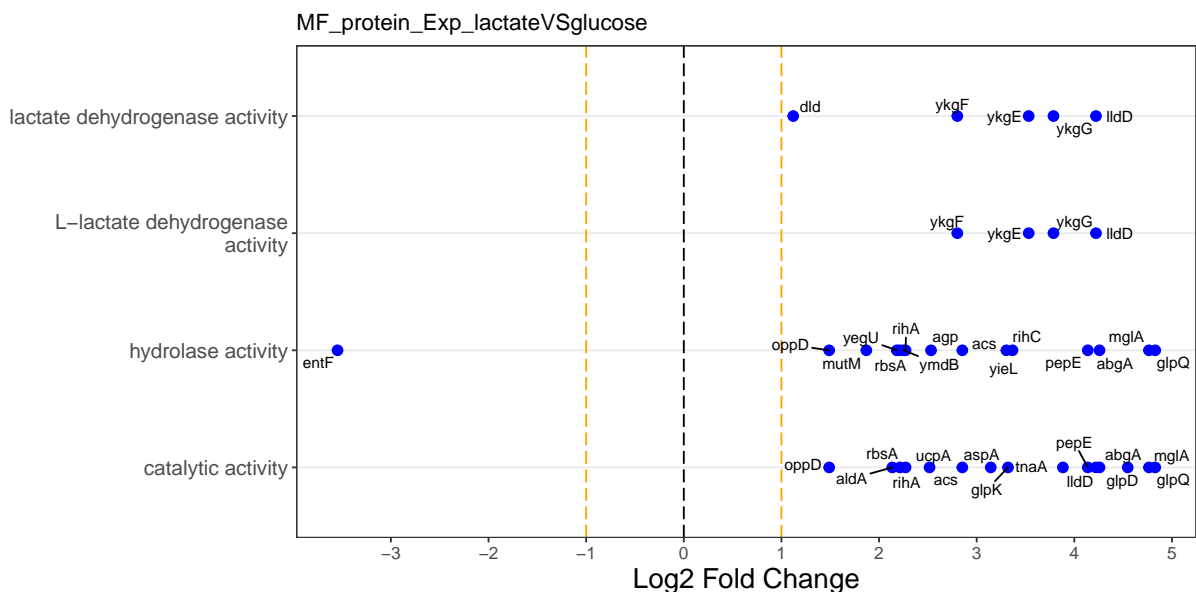


Figure S22: **Significantly differentially expressed GO annotations related with molecular functions and associated genes with lactate as carbon source, as determined by protein abundances in exponential phase.** The top 4 differentially expressed molecular functions are shown along the *y* axis, and the relative fold change of the corresponding genes is shown along the *x* axis. We show up to 10 of the most significantly changed molecular functions and for each molecular function, we show up to 15 of the most significantly changing genes.

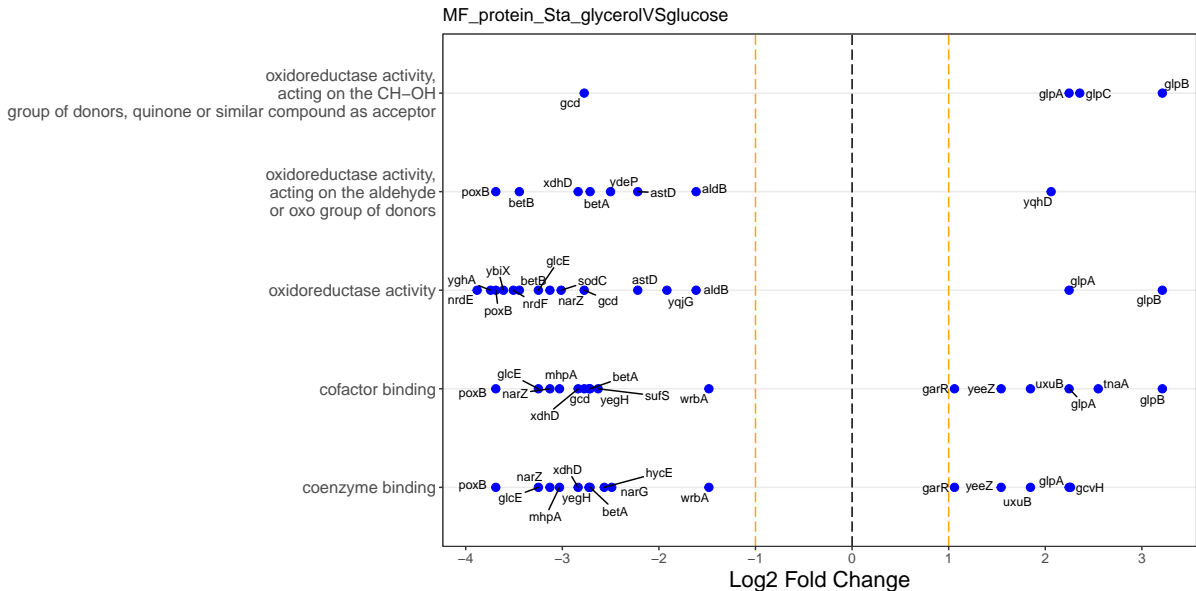


Figure S23: **Significantly differentially expressed GO annotations related with molecular functions and associated genes with glycerol as carbon source, as determined by protein abundances in stationary phase.** The top 5 differentially expressed molecular functions are shown along the *y* axis, and the relative fold change of the corresponding genes is shown along the *x* axis. We show up to 10 of the most significantly changed molecular functions and for each molecular function, we show up to 15 of the most significantly changing genes.

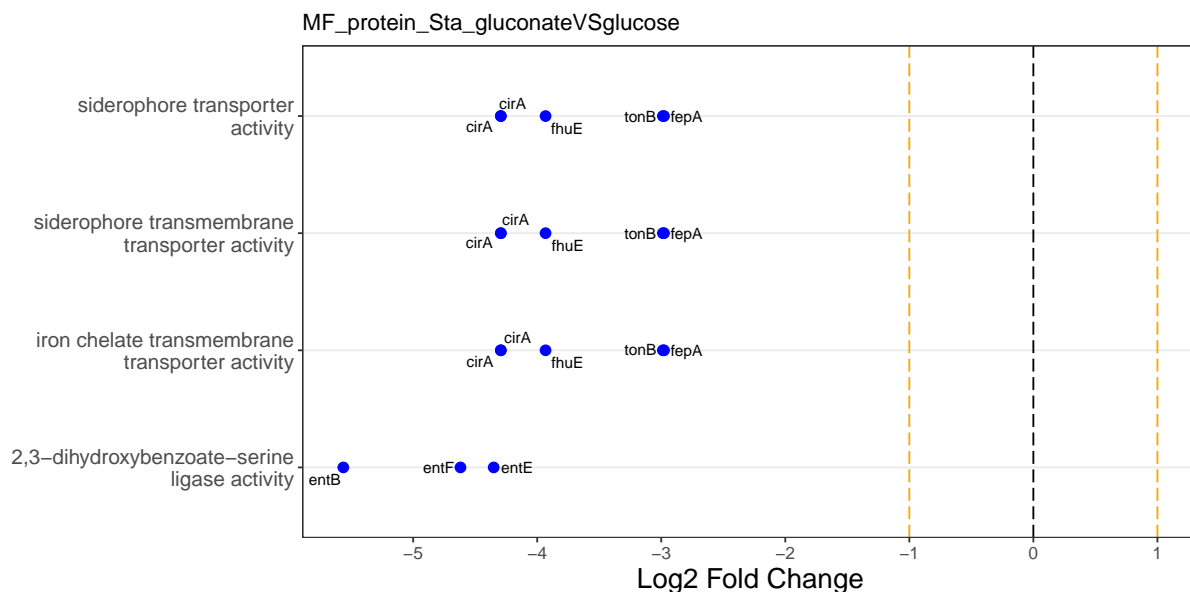


Figure S24: **Significantly differentially expressed GO annotations related with molecular functions and associated genes with gluconate as carbon source, as determined by protein abundances in stationary phase.** The top 4 differentially expressed molecular functions are shown along the *y* axis, and the relative fold change of the corresponding genes is shown along the *x* axis. We show up to 10 of the most significantly changed molecular functions and for each molecular function, we show up to 15 of the most significantly changing genes.

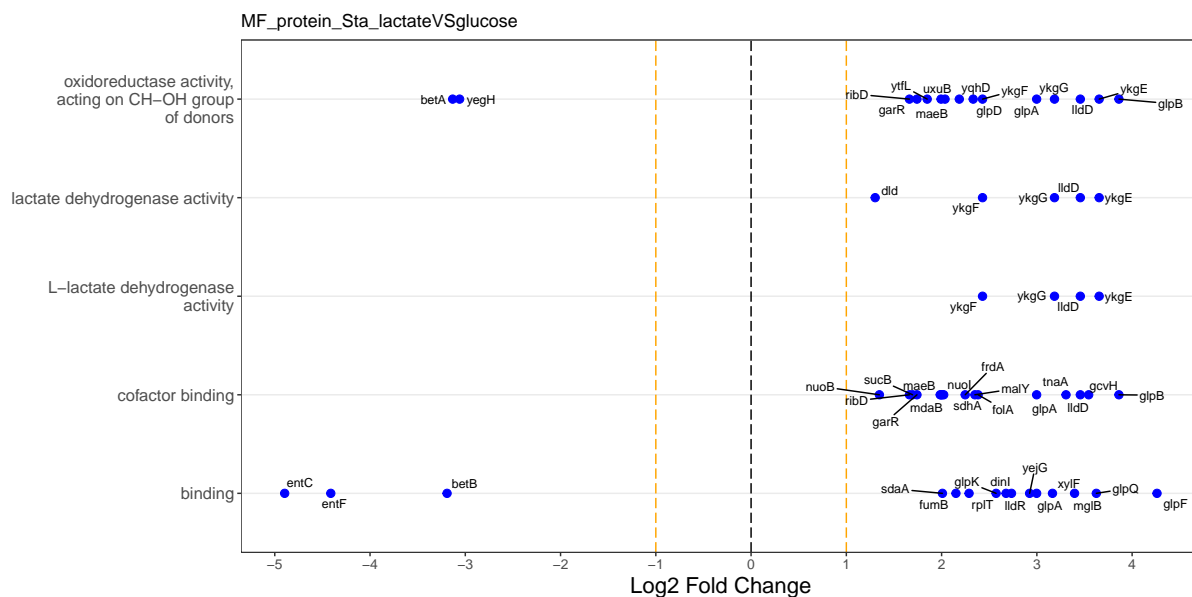


Figure S25: **Significantly differentially expressed GO annotations related with molecular functions and associated genes with lactate as carbon source, as determined by protein abundances in stationary phase.** The top 5 differentially expressed molecular functions are shown along the *y* axis, and the relative fold change of the corresponding genes is shown along the *x* axis. We show up to 10 of the most significantly changed molecular functions and for each molecular function, we show up to 15 of the most significantly changing genes.





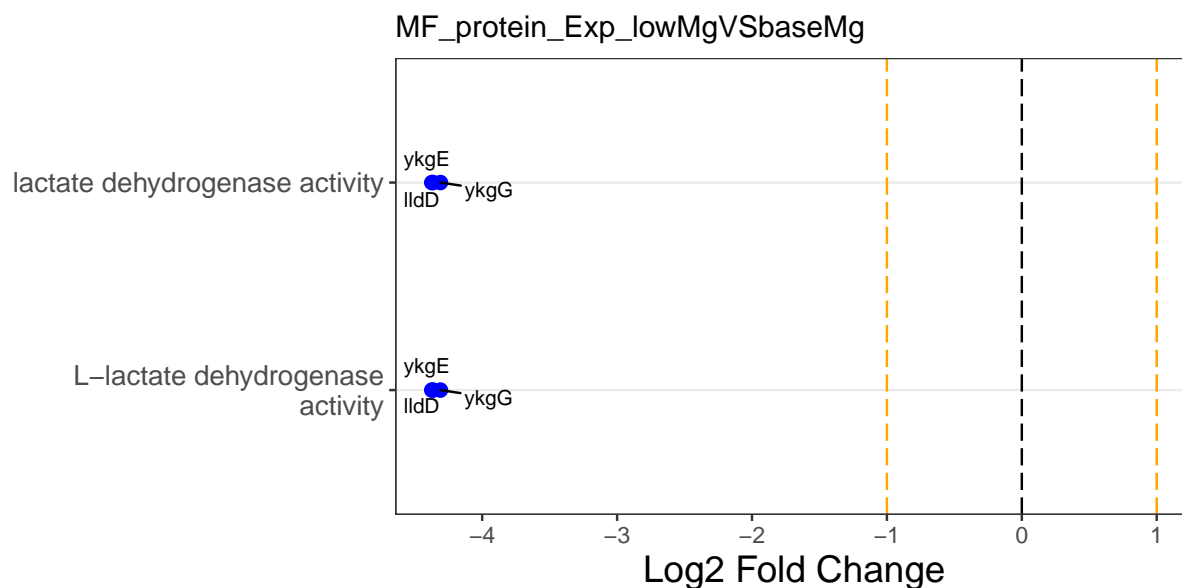


Figure S28: **Significantly differentially expressed GO annotations related with molecular functions and associated genes with low  $Mg^{2+}$  levels, as determined by protein abundances in exponential phase.** The top 2 differentially expressed molecular functions are shown along the  $y$  axis, and the relative fold change of the corresponding genes is shown along the  $x$  axis. We show up to 10 of the most significantly changed molecular functions and for each molecular function, we show up to 15 of the most significantly changing genes.

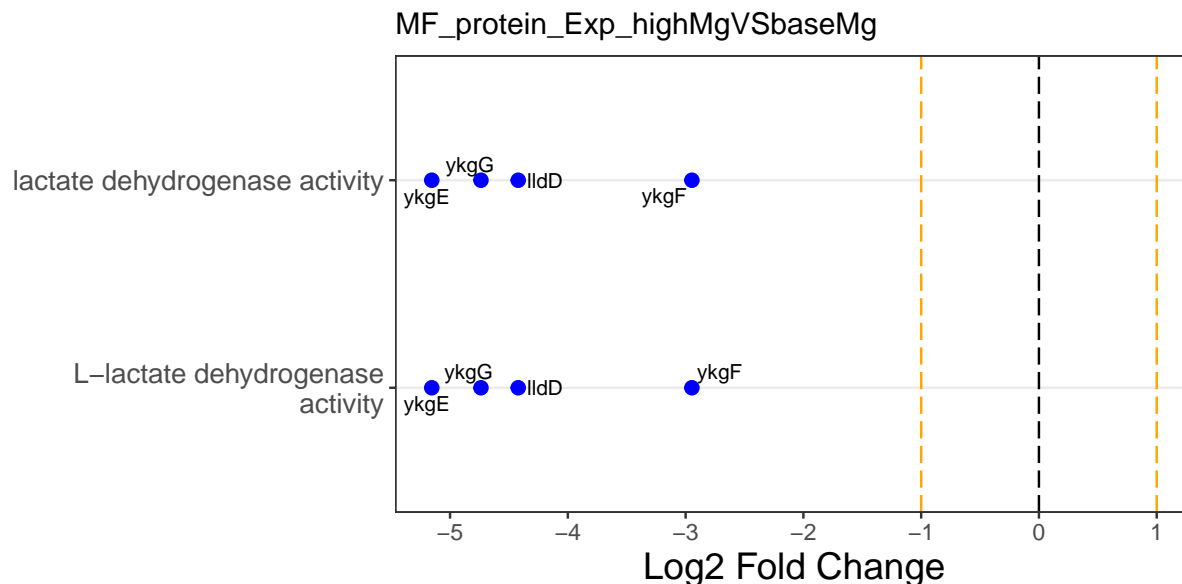


Figure S29: **Significantly differentially expressed GO annotations related with molecular functions and associated genes with high  $Mg^{2+}$  levels, as determined by protein abundances in exponential phase.** The top 2 differentially expressed molecular functions are shown along the  $y$  axis, and the relative fold change of the corresponding genes is shown along the  $x$  axis. We show up to 10 of the most significantly changed molecular functions and for each molecular function, we show up to 15 of the most significantly changing genes.

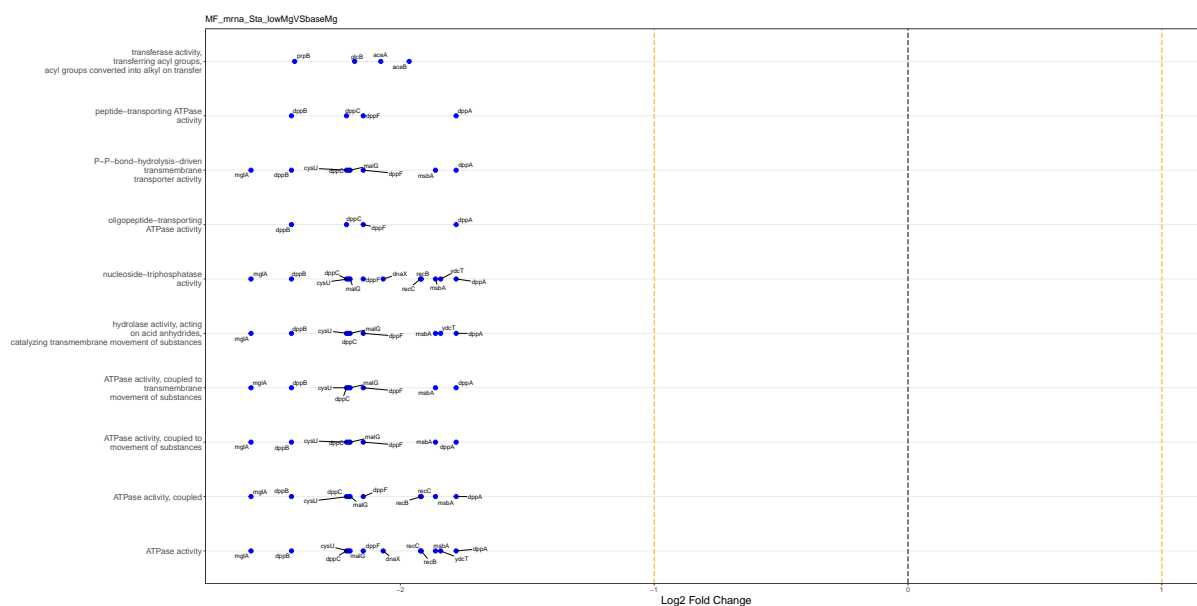


Figure S30: **Significantly differentially expressed GO annotations related with molecular functions and associated genes with low  $Mg^{2+}$  levels, as determined by mRNA abundances in stationary phase.** The top 10 differentially expressed molecular functions are shown along the  $y$  axis, and the relative fold change of the corresponding genes is shown along the  $x$  axis. We show up to 10 of the most significantly changed molecular functions and for each molecular function, we show up to 15 of the most significantly changing genes.

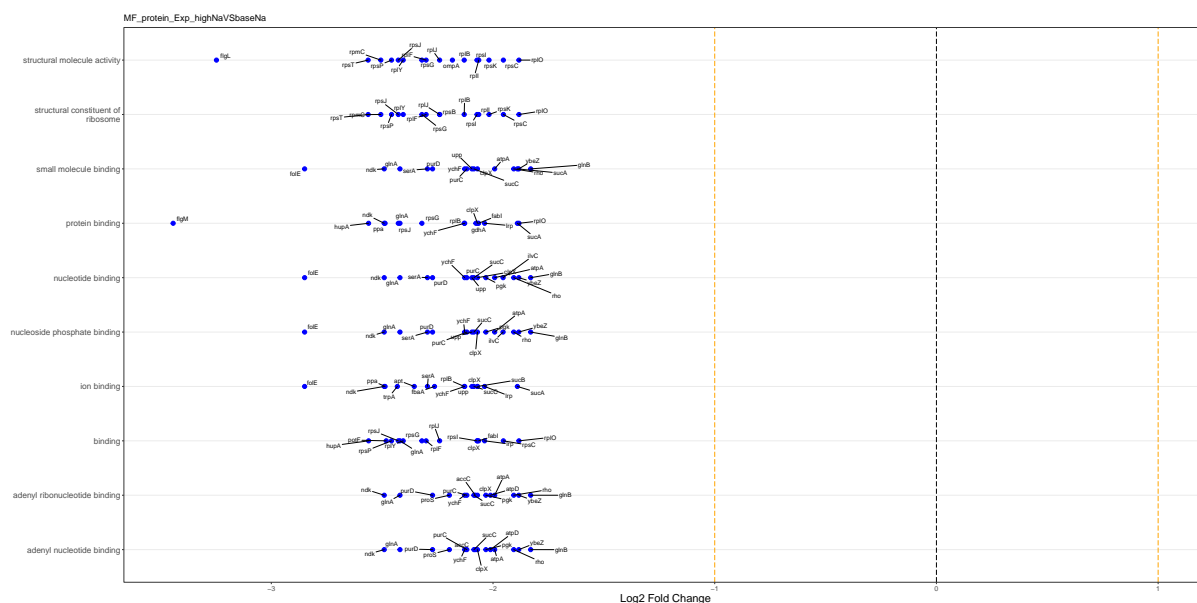


Figure S31: **Significantly differentially expressed GO annotations related with molecular functions and associated genes with high  $Na^{+}$  levels, as determined by protein abundances in exponential phase.** The top differentially expressed molecular functions are shown along the  $y$  axis, and the relative fold change of the corresponding genes is shown along the  $x$  axis. We show up to 10 of the most significantly changed molecular functions and for each molecular function, we show up to 15 of the most significantly changing genes.

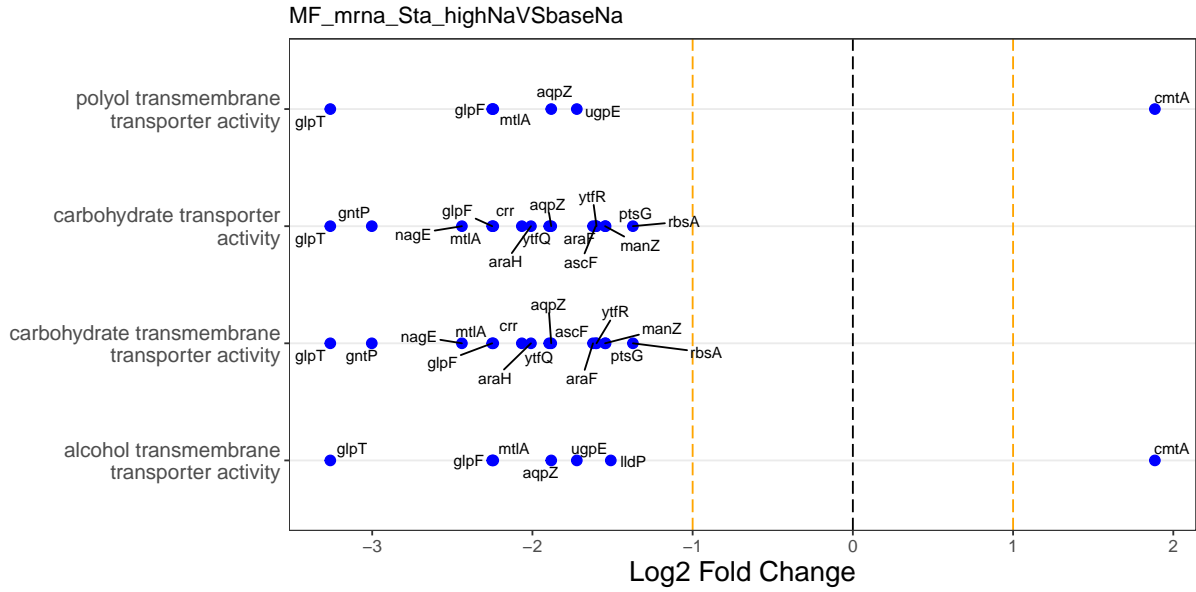


Figure S32: **Significantly differentially expressed GO annotations related with molecular functions and associated genes with high  $\text{Na}^+$  levels, as determined by mRNA abundances in stationary phase.** The top 5 differentially expressed molecular functions are shown along the  $y$  axis, and the relative fold change of the corresponding genes is shown along the  $x$  axis. We show up to 10 of the most significantly changed molecular functions and for each molecular function, we show up to 15 of the most significantly changing genes.

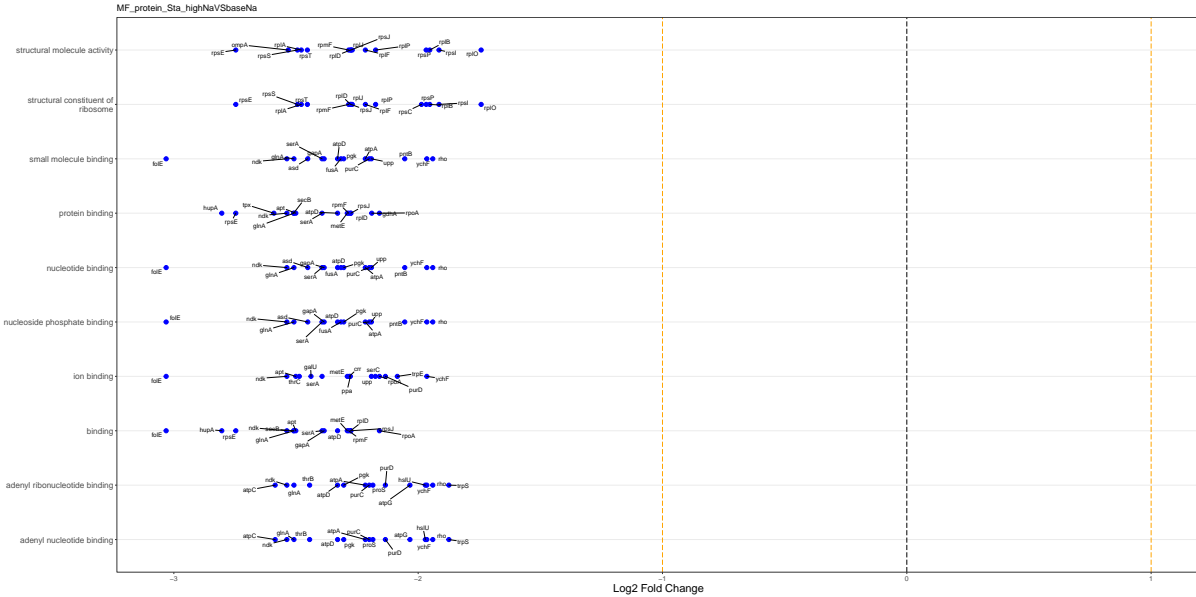


Figure S33: **Significantly differentially expressed GO annotations related with molecular functions and associated genes with high  $\text{Na}^+$  levels, as determined by protein abundances in stationary phase.** The top 10 differentially expressed molecular functions are shown along the  $y$  axis, and the relative fold change of the corresponding genes is shown along the  $x$  axis. We show up to 10 of the most significantly changed molecular functions and for each molecular function, we show up to 15 of the most significantly changing genes.

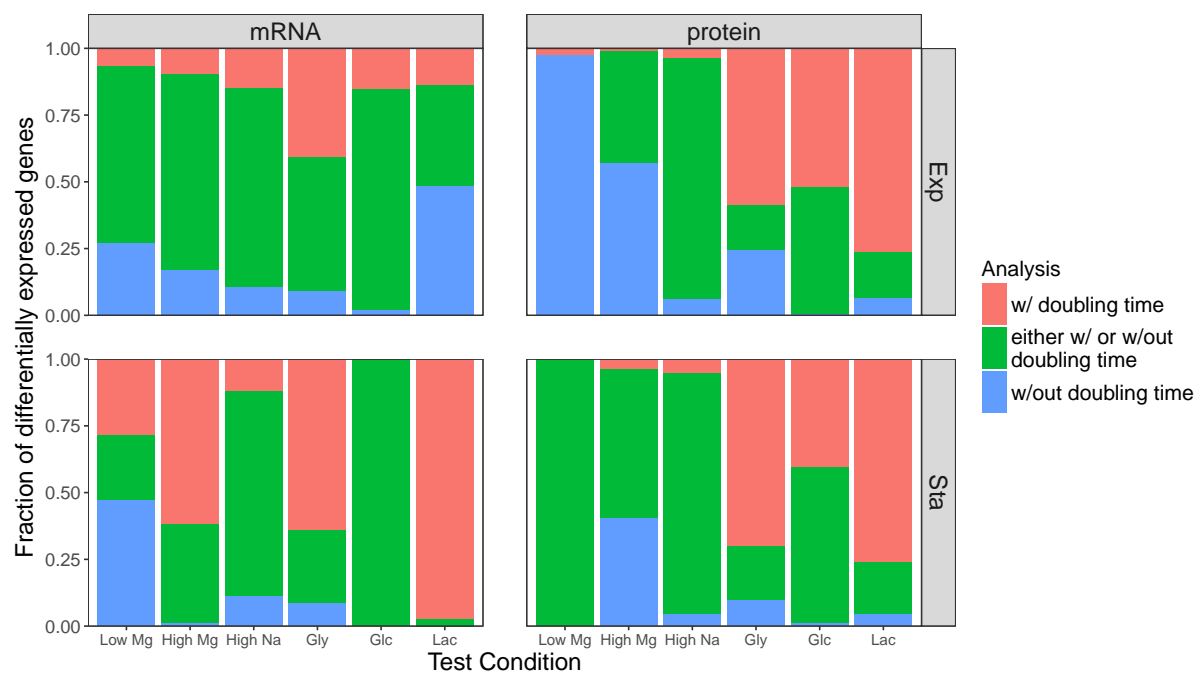


Figure S34: **Fraction of differentially expressed genes that are found in analyses with or without controlling for doubling time.** Shown are the fractions of genes identified as differentially expressed only when controlling for doubling time (red), only when not controlling for doubling time (blue), or in both cases (green). Combined with the absolute numbers of differentially expressed genes in the various conditions (Figure 5), we can see that the main differences in analyses with or without doubling time arise for protein abundances analyzed with respect to different carbon sources.

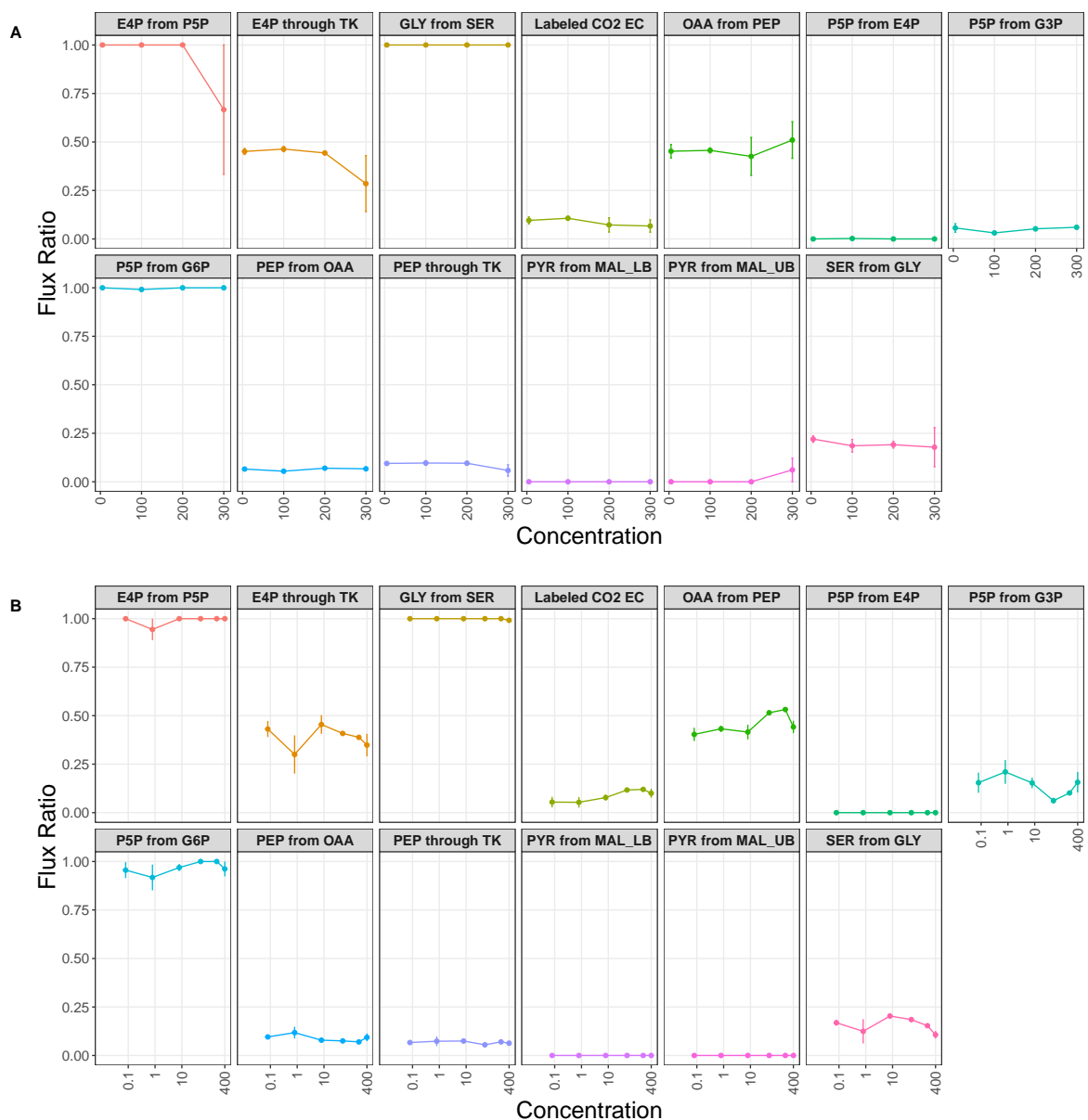


Figure S35: **Flux ratios versus ion concentrations.** 13 different flux ratios were measured with respect to four different Na<sup>+</sup> and five different Mg<sup>2+</sup> concentrations. (A) Concentrations with respect to changing Na<sup>+</sup> concentrations. (B) Concentrations with respect to changing Mg<sup>2+</sup> concentrations. There was no significant trend of increase or decrease in flux ratios with respect to either Na<sup>+</sup> or Mg<sup>2+</sup> concentrations (Supplementary Table 13).

## Supplementary Tables

### Supplementary Table S1

File name: tableS1\_meta\_data.csv

Meta data table that gives information about all samples. Includes information about MURI numbers, experiment name, the time that sample is collected, harvest date, number of RNA samples (tech. replicates), number of protein samples (tech. replicates), batch numbers, Mg<sup>2+</sup>, Na<sup>+</sup> concentrations, growth phase, Mg<sup>2+</sup> and Na<sup>+</sup> levels, growth phases, doubling time related information (mean,  $\pm$ 95% confidence intervals,  $r^2$ )

### Supplementary Table S2

File name: tableS2\_mRNA\_normalized\_raw\_data.csv

mRNA data after normalization with DeSeq2 for size factors. Includes information for 4197 distinct proteins, and for 105 samples

### Supplementary Table S3

File name: tableS3\_protein\_normalized\_raw\_data.csv

Protein data after normalization with DeSeq2 for size factors. Includes information for 4197 distinct proteins, and for 152 samples

### Supplementary Table S4

File name: tableS4\_fluxData.csv

Raw flux data for 13 branches for exponential and stationary phase

### Supplementary Table S5

File name: tableS5\_doubling\_times.csv

Includes doubling time information for different conditions and replicates, and  $\pm$ 95% confidence intervals.

### Supplementary Table S6

File name: tableS6\_clustering\_mrna\_cophenetic.csv

Influence of parameter changes on overall mRNA data. This is measured by clustering scores for individual conditions and sub-conditions including batches for mRNA data

### Supplementary Table S7

File name: tableS7\_clustering\_protein\_cophenetic.csv

Influence of parameter changes on overall protein data. This is measured by clustering scores for individual conditions and sub-conditions including batches for protein data

### Supplementary Table S8

File name: tableS8\_combinedOutputDF\_DeSeq.csv

DeSeq2 enrichment analyse results for all genes and for all distinct tests. Table contains information about :

- Id (ECB number for mRNA and YP number for proteins), and corresponding gene name
- Direct outcomes of DeSeq2 such as base mean value, log2FoldChange, ifcSE, stat, pvalue, padj.
- Direction of the change wrt base level (" +1 " for increase " -1 " for decrease)
- Data type (mRNA or protein) growth phase

- What is tested; base value and contrast.
- Individual output file name
- Carbon Source,  $\text{Mg}^{2+}$  and  $\text{Na}^+$  levels and growth phase of test data
- Control parameters of the test (batch or batch + growth rate)

### **Supplementary Table S9**

File name: tableS9\_combinedDifferentiallyExpressedGenes\_DeSeq.csv

Filtered version of Supplementary Table S8 with  $P < 0.05$  and  $\log_2\text{FoldChange} > 2$

### **Supplementary Table S10**

File name: tableS10\_combinedResultList\_DAVID.csv

The DAVID web service outputs for KEGG and MF tests. Includes information for 24 tests which were controlled for batch effect

### **Supplementary Table S11**

File name: tableS11\_changed\_protein\_carbonSource\_ExpSta.csv

Newly appeared genes when we control for "batch + growth rate" instead of "batch"; for proteins, and tested for carbon source. For both exponential and stationary phase

### **Supplementary Table S12**

File name: tableS12\_changed\_DAVID\_P05.csv

Enriched KEGG pathways and molecular functions based on the genes listed on Supplementary Table S11

### **Supplementary Table S13**

File name: tableS13\_flux\_vs\_conc\_Pvalues.csv

P values obtained by likelihood maximization for flux vs concentration for individual flux branches with individual phase (either exponential or stationary) and with individual salt ( $\text{Mg}^{2+}$  or  $\text{Na}^+$ )

### **Supplementary Table S14**

File name: tableS14\_flux\_vs\_doublingTime\_Pvalues\_tog.csv

P values obtained by likelihood maximization for flux vs doubling time for individual flux branches